

RESEARCH

Open Access



A biocompatible nanoformulation of curcumin analogue and curd exosomes targeting EphA2 signalling cascade in head and neck cancer

Kaumudi Pande^{1,3}, B. K. Bettadaiah^{2,3} and Anbarasu Kannan^{1,3*}

*Correspondence:
anbarasu@cftri.res.in

¹ Cancer and Exosome Biology Laboratory, Department of Biochemistry, CSIR- Central Food Technological Research Institute, Mysuru 570020, India

² Department of Plantation Products, Spices & Flavour Technology, CSIR- Central Food Technological Research Institute, Mysuru 570020, India

³ Academy of Scientific and Innovative Research (AcSIR), Ghaziabad 201002, India

Abstract

Background: Major therapeutic developments have been made in the prevention of head and neck cancer (HNC), and crucial measures have been implemented for the survival of patients. The advent of cancer nano-theranostic as an effective approach targets cancer by allowing drug aggregation at the tumour site, its proper bioaccessibility, and tumour cell death. Curd exosomes are the cellular interactive nanovesicles, considered a convenient conveyance medium for cargoes still unexplored. Curcumin analogue alanine is primarily recognised for its superior radical scavenging activity and anti-mutagen properties compared with curcumin.

Methods: The current study focussed on the isolation and characterisation of curd exosomes, followed by their interaction with cancer cells to deliver their content conveniently. Herein, we developed a nanoformulation of curd exosomes loaded with curcumin alanine to determine its bioaccessibility and anti-proliferative effect compared with curcumin alanine free drug. In addition, the influence of curcumin alanine and its nanoformulation on cell morphology, nucleus structures, colony formation potential, and tumour cell death was observed. The expression of EphA2 and its associated molecules was determined using western blot and PCR to explore the mechanism at the cellular level.

Results: The recent investigation revealed the encapsulation of curcumin analogue alanine in curd exosomes enhanced the bioaccessibility in contrast with curcumin alanine. Then, we focussed on the curcumin alanine effect on HNC cells to monitor morphological alterations, a reduction in cell multiplication, and triggering apoptosis. Particularly, we found considerable suppression of EphA2 influencing mitochondrial dynamics with the strengthening of mitochondrial fusion MFN1 and MFN2, whereas fission-associated protein DRP1 was down-regulated by the treatment of curcumin alanine nanoformulation. Furthermore, curcumin alanine nanoformulation activates the apoptotic marker caspase-7 and suppresses the anti-apoptotic marker Bcl-xL.

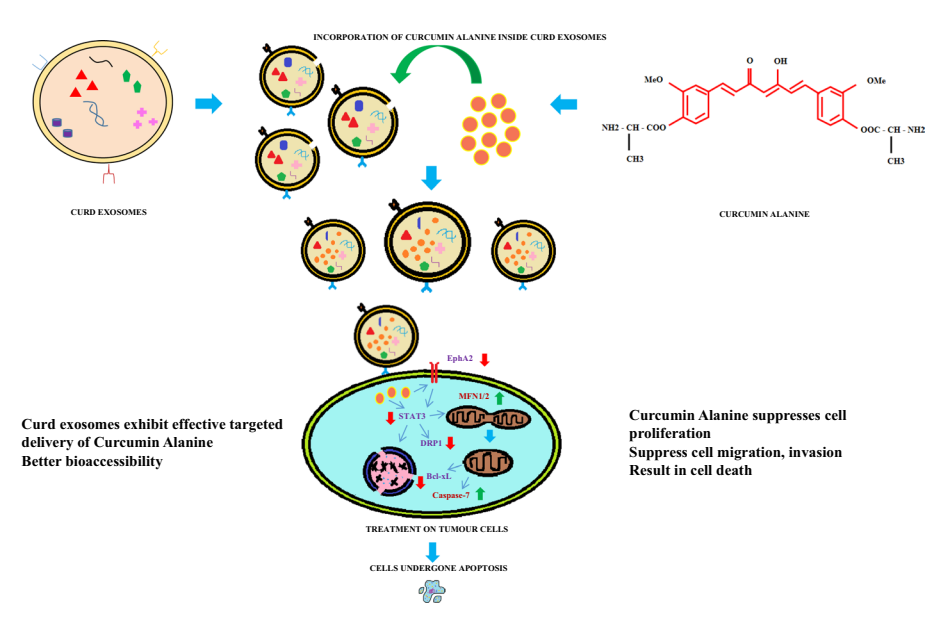
Conclusion: Hence, these findings have drawn attention to curd exosomes loaded curcumin alanine nanoformulation impairing cell multiplication and mitochondrial



fission, leading to apoptotic cell death, as one of the effective approaches for the treatment of HNC.

Keywords: Head and neck cancer, Curcumin alanine, Exosomes, EphA2, Mitochondrial dynamics

Graphical Abstract



Background

Curcumin(CUR) is a yellow polyphenolic element present in the roots of the turmeric plant, exhibiting diverse functions valuable to mankind. According to the Global Market Report, there will be an anticipated expansion of the curcumin market size to 141.94 million USD in 2023, with an estimation of 220.4 million USD (9.2% growth) until 2028 (Curcumin Market 2023). In India, turmeric has been employed for the treatment of chronic diseases in Ayurveda since ancient times. As stated in the Statistica report, Maharashtra generated 278 thousand metric tonnes of turmeric, making it the leading state, followed by Telangana and Rajasthan, in the financial year 2023 (Sandhya Keelery 2023). It can be employed for the treatment of cystic fibrosis, diabetes, epilepsy, arthritis, Parkinson’s, and various skin allergies. Curcumin is known to regulate various signalling mechanisms, which include cancer tumorigenesis, lipid peroxidation, GPCR, and the TNF pathway (Aggarwal et al. 2007). In addition, curcumin was known to undergo adjuvant therapy with resveratrol, targeting cancer-induced cachexia-regulating sirtuin-1 protein. Curcumin exerts an anti-microbial effect by suppressing the growth of *Pseudomonas aeruginosa* and *Streptococcus mutans* (Porro and Panaro 2023). It was noteworthy that curcumin acts as an anti-inflammatory agent towards wound healing in myofibroblasts, which allows remodelling for wound contraction and its closure. Curcumin suppresses inflammation at an initial stage, thereby increasing cytokine production and triggering the NF-κβ mechanism in the wounded area (Barchitta et al. 2019). Moreover, curcumin acts as

an anti-cataract agent by upholding lens Ca^{2+} ATPases and regulating calcium ions. In terms of an in vivo study, curcumin was found to be successful in inhibiting cataractogenesis at an effective dosage of 8 g per day for 3 months. Therefore, it can be considered a therapeutic molecule for the eyes (Thiagarajan and Manikandan 2013). Curcumin reverses doxorubicin resistance in breast cancer by inhibiting NF- κ B which releases p300 transcription co-activator to bind with p53 and activates the apoptosis mechanism. Moreover, cancer stem cells demonstrate insusceptibility towards the standard cancer treatments was inhibited by curcumin reducing the CD44 levels and preventing the phosphorylation of STAT3 in breast cancer (Kubatka et al. 2024).

Despite various biological attributes, curcumin exhibits low bioavailability, with 0.051 $\mu\text{g}/\text{mL}$ from 12 g of curcumin content found in plasma and a major portion eliminated from the body (Liu et al. 2016). To solve this complexity, curcumin analogue has been developed by conjugation of curcumin with the predominant amino acid alanine, forming 1,7-Bis(4-*O*-L-alaninoyl-3-methoxyphenyl)-1,4,6-heptatriene-5-ol-3-one. The synthesis deals with the chemical reaction of curcumin with 4-dimethylaminopyridine, triethylamine, and *N,N'*-dicyclohexylcarbodiimide in the presence of dioxane in a nitrogen environment. The curcumin analogue alanine (CAA), obtained with a yield of 76% and a melting point of 133–135 °C, exhibits enhanced anti-oxidant activity and anti-mutagenicity ability as compared with curcumin (Parvathy et al. 2010). In the current study, we aimed to explore the decelerating growth of head and neck cancer cells by exposure to CAA nanoformulation with attention to the EphA2 signalling cascade.

Curd and fermented milk products are known for their versatile role in strengthening the immune system, preventing obesity, and providing vital minerals to the body. Its synthesis is based on the fermentation procedure carried out by *Lactobacillus* sp., which contains the lactase enzyme for the breakdown of lactose sugar in milk into glucose and galactose for the production of lactic acid. Further, *Lactobacillus* bacteria divide rapidly at room temperature. Lactic acid enables the coagulation of milk by denaturing the casein milk protein to a fibrous, thick nature, thus changing the pH of milk towards the acidic range. This phenomenon results in the separation of aqueous (whey) from semi-solid content, known as curdling (Okada et al. 2009). Curd helps in targeting foreign particles, thereby maintaining a healthy stomach; moreover, it reduces oral diseases in the presence of a wide spectrum of beneficial bacterial strains (Balaganesh et al. 2022). Curd has been considered an important component of *Panchgavya* therapy that provides immense health benefits, including the prevention of skin infections, heart diseases, and vitamin deficiencies, and is considered an excellent blood purifier (Bajaj et al. 2022). The probiotic enrichment in curd, comprising non-haemolytic lactic acid bacteria strains, exhibited anti-microbial activity against pathogens; subsequently, curd emerged as a perfect candidate for functional food production (Khushboo and Malik 2023).

Exosomes are a kind of extracellular nanovesicles comprising a plethora of biomolecules, which include nucleic acids, proteins, fats, carbohydrates, and metabolites. Its spherical shape depicts uniformity similar to exosomes isolated from different sources and a buoyant density of 1.13–1.21 g/mL observed under a transmission electron microscope (Feng et al. 2021). Prior studies indicated that exosomes comprised of tumour suppressor lncRNAs that modulate angiogenesis in tumour cells. These exosomes transfer lncRNA GAS5 which triggers PTEN expression, thereby, suppressing PI3K/Akt pathway

in the lung cancer cells. On the other hand, tumour-associated macrophages-derived exosomes exhibit a higher level of miR-29a-3p and miR-21-5p leading to an imbalance between Tregs and Th17 cells affecting STAT3-promoting tumorigenesis in epithelial ovarian carcinoma (Paskeh et al. 2022). Therefore, the behaviour of the exosome function relies on its parent cell from where it originates. In recent decades, the nanomedicine area has shown tremendous progress, focussing on a broad range of ailments. The mesenchymal stem cells obtained exosomes influence glucose and lipid metabolism through glycolytic enzymes and transporters GLUT1 and GLUT4 for the remedy of diabetes mellitus (Ashrafizadeh et al. 2022). The introduction of synthetic miR-200a mimics into mesenchymal cell exosomes and their subsequent treatment on AGS cells increases E-cadherin, along with the decrease in the expression of β -catenin, ZEB1, Snail1, and vimentin growth associated molecules targeting gastric cancer (Mirzaei et al. 2023). Exosomes have the major function of cellular communication and aid in the effortless transfer of cargo to the cells. Casing the cargoes inside its lipid bilayer prevents their degradation and helps them cross the blood–brain barrier. Its formation occurs inside the cell by endosomal membrane budding, followed by the loading of diversiform molecules at different stages by ESCRT components, and eventually release from the plasma membrane to the extracellular space (Gurung et al. 2021). In the present study, exosomes derived from curd were utilised as a curcumin analogue alanine delivery vehicle, followed by treatment on HNC cell lines. The interaction of curd exosomes with the target cells will be further analysed and considered for effective conveyance and to minimise the excess of drugs that usually show better outcomes.

Head and neck cancer (HNC) is considered a severe kind of tumour that appears in the mouth, nasal cavity, and throat and extends to the neighbouring organs. It emanates from mucosal epithelial cells that have transformed their conventional physiology by exposure to harmful chemicals or radiation. This modification may occur at the gene and protein levels, thereby interrupting the typical signalling mechanism of healthy cells. The incidence rate of HNC in India was 25.9 and 8.0 per 100,000 population for males and females, respectively. However, the proportion of HNC to all-site cancer in other countries such as the USA, UK and Australia were 4.3%, 3.7% and 4.0%, respectively, for males and less than 2% for females (Bagal et al. 2023). The mortality estimation of HNC cases by the Global Burden of Disease study was 705,901 by the year 2030, with a percentage increment of 38% from the year 2016 to 2030. Over and above, there were 176,534 mortality cases predicted in Southeast Asia and neighbouring regions with increasing economic loss (Patterson et al. 2020). Histopathology and surgery emerged as reliable methods for the detection and removal of tumour tissues from the body (Folz et al. 2008; Cohen et al. 2018). The major possibilities for developing HNC include tobacco and alcohol consumption, the human papillomavirus, nutrition, and the oral microenvironment. This leads to genomic instability, drug resistance, inflammation, and tumour growth, which eventually disperses to distinct organs (Miranda-Galvis et al. 2021). The patients of HNC underwent difficulty dealing with the pain and survival rate. Depending upon the choice of treatment required by the patient, there are robotic surgery, immunotherapy, targeted drug therapy, radiotherapy, and chemotherapy that lower the risk of mortality (Kaidar-Person et al. 2018). Mitochondrial dysfunction impaired

mitochondrial function affecting mitochondrial fission and fusion events in cancer. Mitochondrial dynamics maintain the count, shape alteration, and positioning of mitochondria in the cell. Mitochondrial fission involves the splitting of mitochondrion into two separate mitochondria, a process controlled by DRP1 present in the cytoplasm which moves along the outer surface of mitochondria for incision. Conversely, mitochondrial fusion is the merging of mitochondria into a single large mitochondrion regulated by MFN1 and MFN2 (Caron and Bertolin 2024). Cancer involves an imbalance of fission and fusion events.

Erythropoietin-producing hepatocellular receptor 2, or Ephrin type-A receptor 2 (EphA2), is a tyrosine kinase-related receptor with an extracellular cysteine-rich cell surface glycoprotein involved in neural system development. Its gene localization on chromosome 1p36 is a single transmembrane protein that oligomerizes to stimulate kinase activity, and its phosphorylation promotes growth and blood vessel formation (Xiao et al. 2020). The conventional role of EphA2 involves embryonic advancement and regulates bone remodelling (Irie et al. 2009). Previous reports stated that EphA2 is associated with extracellular matrix protein and enhanced focal adhesion activity by fibronectin deposition (Finney et al. 2021). The main focus of our work with CAA is to explore its anti-proliferative effect on HNC cells through its exosomal formulation and clarify its influence on the EphA2 signalling mechanism for the development of anti-tumour drugs.

Materials and methods

Cell culture and reagents

Head and neck cancer cell lines KB-3-1 and HEP-2 were purchased from NCCS Pune, India, and grown in cultured media Dulbecco's modified Eagle's medium (DMEM) and Minimum essential media (MEM) (Sigma-Aldrich Chemicals) added with sodium bicarbonate (Himedia Laboratories Private Limited), and 10% v/v Foetal bovine serum (Gibco Thermofisher Scientific) under 5% CO₂ at 37 °C. Curcumin analogue Alanine was obtained from the Department of Plantation Products, Spices & Flavor Technology, CSIR-Central Food Technological Research Institute, India. Cow milk and curd as a starter were purchased from the local market in Mysuru, India. Polyethylene glycol 6000 (PEG), curcumin, fungal amylase, pepsin, bile salt, pancreatin, ethidium bromide (EtBr), and acridine orange (AO) were purchased from Himedia Laboratories Private Limited. MTT (3-(4,5-dimethylthiazol2-yl)-2,5-diphenyltetrazolium bromide), and 3,3'-diiodoacryloxycarbocyanine perchlorate (DiO) were obtained from Sigma-Aldrich chemicals. DAPI (4',6-diamidino-2-phenylindole) was obtained from Abcam. The antibodies, such as EphA2 (#6997), Bcl-xL (#2762), β-actin (8H10D10 #3700), Caspase-7 (#9492), STAT3 (#12640), and HRP-conjugated antibodies Mouse (#7076) and Rabbit (#7074) were purchased from Cell Signaling Technology. In addition, the phosphorylated antibody EphA2 (AP10821) was purchased from ABclonal. The antibodies DRP1 (AB54088), and MFN2 (AB56889) were purchased from Abcam.

Curd exosomes preparation

Curd was prepared by milk fermentation, mixing, and incubation at room temperature for a day. To isolate curd exosomes, the curd was collected in tubes in a 50 ml falcon tube and centrifuged at 7000 rpm at 4 °C for 20 min. In the ultracentrifuge tube, 30 ml of the supernatant was collected, followed by the first round of ultracentrifugation at 100,000×g for 1 h at 4 °C to remove large macrovesicles and transfer the supernatant in a second tube for the second round of ultracentrifugation at 150,000×g for 90 min at 4 °C to acquire exosomes. The supernatant was discarded, and the curd exosomes pellet was resuspended in phosphate buffer saline (PBS), filtered using a 0.2-micron syringe filter, and stored at – 80 °C (Ansari et al. 2024).

Characterisation of curd exosomes

Curd exosomes were defined by their morphology using transmission electron microscopy (TEM), scanning electron microscopy (SEM), dynamic light scattering (DLS), protein content determination using SDS gel, and lipid content by gas chromatography–mass spectrometry (GC–MS). The conventional morphology of curd exosomes was examined using TEM and SEM (Fakhredini et al. 2022). The exosomes were fixed with 1% glutaraldehyde followed by dehydration with ethanol, and visualised by TEM (Leo, Zeiss, Germany). In addition, the structure of exosomes was examined using SEM by fixing with paraformaldehyde and washed with varied concentrations of ethanol (70%, 90%, and 100%). The sample was loaded on a silicon chip and coated with gold for observation under the SEM (Leo, Zeiss, Germany). The size distribution and stability of curd exosomes were measured using a Malvern zetasizer instrument by diluting curd exosomes in 1 mL of PBS and transferring them into a glass cuvette with a round aperture, on the other hand, for zeta potential, 1 mL of MilliQ water was taken as a dispersant for analysis using a clear disposable U-shaped capillary tube. The temperature equilibration was 25 °C with a refractive index of 1.33 for both the dispersant and 0.88 viscosity. The peak intensity depicts the size and zeta potential distribution of exosomes (Shariati et al. 2021). The curd exosomes are composed of diverse kinds of proteins present in their lipid bilayer along with their lumen. Therefore, curd exosomes protein was evaluated using a nanodrop spectrophotometer and further separated on SDS gel, which was visualised using a Coomassie R-250 staining solution for protein band dyeing (Sedykh et al. 2017). The lipid composition of curd exosomes was estimated by a simple protocol of Folch extraction using methanol, chloroform, and orthophosphoric acid, thereby enabling minor modification (Folch et al. 1957). The consecutive rounds of lipid isolation by solvents were followed by centrifugation at 12,000 rpm for 5 min at 4 °C. The lipid sample was kept for evaporation in a high-speed vacuum concentrator for 3 h. The lipid content was determined using thin-layer chromatography for polar and non-polar lipids in curd exosomes. The phospholipid solvent system involved chloroform: methanol:acetone:glacial acetic acid:water in a (10:2:4:3:1) ratio and neutral lipids solvent composed of petroleum ether:diethyl ether:glacial acetic acid in a (7:3:0.1) ratio; thereby, the TLC plates were exposed to iodine vapours. The plate images were taken in the Bio-Rad Gel doc system (Frederik and Broekhoven 1978; Counihan et al. 2010).

Fatty acid analysis was performed by GC–MS using the Agilent Technologies GC system with Mass Hunter Data Acquisition. The GC–MS analysis of the fatty acid methyl

esters (FAMES) of curd exosomes was carried out by processing with C17 internal standard and boron trifluoride, further mixed with n-Hexane and water to obtain fatty acid layer separation. The sample was passed through anhydrous sodium sulphate to remove moisture content and poured into a GC auto-sampler vial (Nguyen et al. 2015).

DiO staining of curd exosomes

The circulating exosomes were analysed in vitro by labelling them with the fluorescent dye 3,3'-Dioctadecyloxycarbocyanine perchlorate (DiO), which allows communication with head and neck cancer cells. The curd exosomes were incubated with DiO dye for incubation at 4 °C in the dark. The labelled exosomes were centrifuged at 13,000 rpm for 20 min at 4 °C to pellet down excess DiO stain. The supernatant containing labelled exosomes was mixed with media and treated on KB-3-1 and HEp-2 cells for 24 h of incubation at 37 °C. On the following day, the cells were washed with PBS and visualised under a fluorescent microscope (Yang et al. 2021).

Preparation of curcumin analogue alanine loading into curd exosomes

In the current study, the design of the experiment determined the internalisation of CAA into curd exosomes using a probe sonicator with slight variation (Wang et al. 2021a, 2021b). Briefly, 500 µg of CAA was mixed with 1.5 mg of curd exosomes that were sonicated at 2-s on-off cycles 15 times and incubated for 1 h at 4 °C. Subsequently, the sonicated sample was centrifuged at 14,000 rpm for 30 min at 4 °C. The CAA-loaded exosomes were stored at - 80 °C, and the evaluation of the concentration of CAA incorporated inside curd exosomes was determined by drug entrapment efficiency and encapsulation efficiency at 423 nm absorbance (Yuan et al. 2022).

Curcumin analogue alanine bioaccessibility

The in vitro gastrointestinal intake of CAA was determined by its bioaccessibility analysis and then HPLC (Dundar et al. 2022). The present study illustrates the difference in usability among curcumin, CAA, and CAA-loaded curd exosomes digestion by treating distinct digestive enzymes. The group samples were processed with fungal amylase (pH 7), pepsin (pH 2), and intestinal juices (pH 7). They were added with acetonitrile, methanol, and water, followed by HPLC analysis with a mobile phase of 70% methanol using a C18 reverse phase column. The absorbance of 423 nm was measured for each sample at isocratic elution (Anubala et al. 2014).

Cytotoxicity of CAA on head and neck cancer

The MTT assay was performed to analyse the cytotoxic impact of curcumin alanine. KB-3-1 and HEp-2 cells were grown in 96-well plates for 24 h and treated with CAA and curd exosome-loaded with CAA for 24 and 48 h. The cells were treated with a 5 mg/mL MTT solution for 3 h. After the addition of DMSO, the absorbance was measured at 570 nm on an ELISA plate reader (Sun et al. 2019).

FTIR spectrum analysis of CAA

The comparative analysis of the structure of curcumin, curd exosomes, curcumin alanine and nanoformulation was carried out using the FTIR Tensor II Bruker instrument.

The samples were prepared in PBS loaded on the transparent crystal and measured in the transmission mode with the wave number ranging from 4000 to 400 cm^{-1} (Zhao et al. 2015).

Cell and nuclear morphology study

To characterise the changes in cell morphology, KB-3-1 and HEp-2 cells were cultured in a 6-well plate for 24 h until the cells adhered and attained morphology. The CAA treatment group, curd exosomes loaded CAA treatment group, and control group were set. After 48 h of treatment, the cells were washed with PBS, and images were taken under an inverted microscope.

For nuclear morphology, the cells were fixed using paraformaldehyde, permeabilised by triton X 100, and then incubated with DAPI fluorescent dye for 10 min. The images were visualised under a fluorescent microscope (Sun et al. 2014).

Clonogenic assay

The HNC cells KB-3-1 and HEp-2 were seeded into petri plates at a density of 2×10^4 cells per plate for 24 h. The cells were treated with CAA, and exosomes were loaded with CAA for 48 h. After the treatment, the cells were washed, fresh media was added, and the plates were kept in the incubator for growth to form colonies. The cultures were fixed using a cell fixation solution and stained with crystal violet for 10 min. The cultures were then washed with water, dried, and images were taken. The colonies were counted (Zhang et al. 2019).

AO-EtBr assay

The dead and alive assay was performed using acridine orange and ethidium bromide at an equal concentration on the head and neck cancer cells. The KB-3-1 and HEp-2 cells were seeded in 6-well plates and treated with CAA and curd exosomes loaded with CAA for 48 h. Further, the cells were stained with fluorescent dyes added in PBS for 5 min and examined by a fluorescent microscope (Teekaraman et al. 2019).

Western blot

The HNC cells KB-3-1 and HEp-2 were seeded on the petri plates, then treated with CAA, and curd exosomes loaded with CAA for 48 h. The protein was extracted using lysis buffer added with PMSF and further centrifuged at 14,000 rpm for 30 min at 4 °C. The protein supernatant was quantified by a nanodrop spectrophotometer, and the total protein was separated on SDS gel and transferred to a PVDF membrane at 25 V and 0.1 amperes for 35 min using a Bio-Rad transblot instrument. The PVDF membrane was processed with slight modification (Wu et al. 2021) by overnight incubation with 3% BSA blocking buffer at 4 °C; moreover, it was incubated with primary antibodies EphA2, phosphorylated EphA2, DRP1, MFN2, STAT3, Bcl-xL, and Caspase-7 for 1 h on the rocker. β -Actin was used as an internal control, followed by incubation with secondary antibodies (rabbit or mouse) for about 1 h at room temperature. The membrane was washed with TBST and observed by the Bio-Rad Chemidoc instrument after treatment with ECL solution.

RNA isolation and reverse transcription PCR

The total RNA was isolated using the Triazol isopropanol method (Haji et al. 2019), with quantification using a nanodrop spectrophotometer. For cDNA conversion, RNA was used as a template along with the reverse transcriptase enzyme according to the kit protocol. The PCR was carried out for EphA2 (5′ GGCAAGGAAGTGGGACCTGAT 3′ and 5′ GGTCGCCAGACATCACGTTG 3′), DRP1 (5′ GAGAAGAAAATGGGGTGGAA 3′ and 5′ GATGAATTGGTTCAGGGCTT 3′), MFN1 (5′ ACACCATTCTAGGAA TTTGC 3′ and 5′ GGCTTCAATGGCCTAGTGTT 3′), MFN2 (5′ CAGCAGAGGCGT AAGGAGTA 3′ and 5′ CGAGAGAAGAGCAGGGACAT 3′), Caspase-7 (5′ GGGTTG AGGATTCAGCAAAT 3′ and 5′ TCGCATGGTGACATTTTTTCT 3′), Bcl-2 (5′ ATG ACTGAGTACCTGAACCG 3′ and 5′ AGCAGAGTCTTCAGAGACAG 3′), STAT3 (5′ TTATCTGTGTGACACCAACG 3′ and 5′ CAAAGGTGAGGGACTCAAAC 3′), and GAPDH (5′ AAGCCTGCCGGTGACTAAC 3′ and 5′ GCATCACCCGGAGGAGAA AT 3′). All the reactions were performed with denaturation at 95 °C for 30 s, specific annealing temperature for respective primers for 45 s, extension at 72 °C for 1 min, and storage at 4 °C. The PCR products were observed on an agarose gel (Fang et al. 2014).

Statistical analysis

The results were shown as mean ± standard deviation (SD). For all the statistical analyses, the *P* value < 0.05 was statistically significant, and graphical data were analysed using Image J and GraphPad Prism software 9.0.

Results

Extraction and physical characterisation of curd exosomes

Curd was prepared from cow milk by the curdling process (Fig. 1A) and was taken for centrifugation to obtain the supernatant to separate the pellet. The centrifugation was carried out at high speed in two rounds to obtain the exosomal pellet of weight 0.9 gm (Fig. 1B). Curd exosomes showed a spherical shape with a size lesser than 200 nm in large numbers observed using TEM (Fig. 1C). Similarly, the SEM image revealed small size sphere vesicles with the intact membrane (Fig. 1D).

The polydispersity index of exosomes was 0.321, depicting the regular size distribution with a peak intensity of size 164.4 nm, and an average size of 114.6 nm (Fig. 1E). The stability of exosomes was determined by their zeta potential, which was approximately − 21.2 mV at 25 °C with a conductivity of 0.586 mS/cm (Fig. 1F). The dynamic light scattering depicts measurements of the nanovesicles exhibiting Brownian movement in suspension (Yang et al. 2018) and undergoing repulsion among each other by the negative charge on their lipid bilayer (Midekessa et al. 2020). The SDS gel depicted different exosomal proteins separated according to different molecular weights (Fig. 1G). To explore further the lipid content of exosomes, TLC was performed by taking different solvent systems that showed prominent bands of phospholipids comprising phosphatidylserine [Rf 0.835] along with a faint band of phosphatidylcholine [Rf 0.67] mentioned in Fig. 1H. Moreover, there were prominent bands of neutral lipids, which include cholesterol [Rf 0.29], free fatty acid [Rf 0.58], methyl ester [Rf 0.84], and cholesterol ester [Rf 0.97], as shown in Fig. 1I. In our study, we investigated the presence of fatty acids in

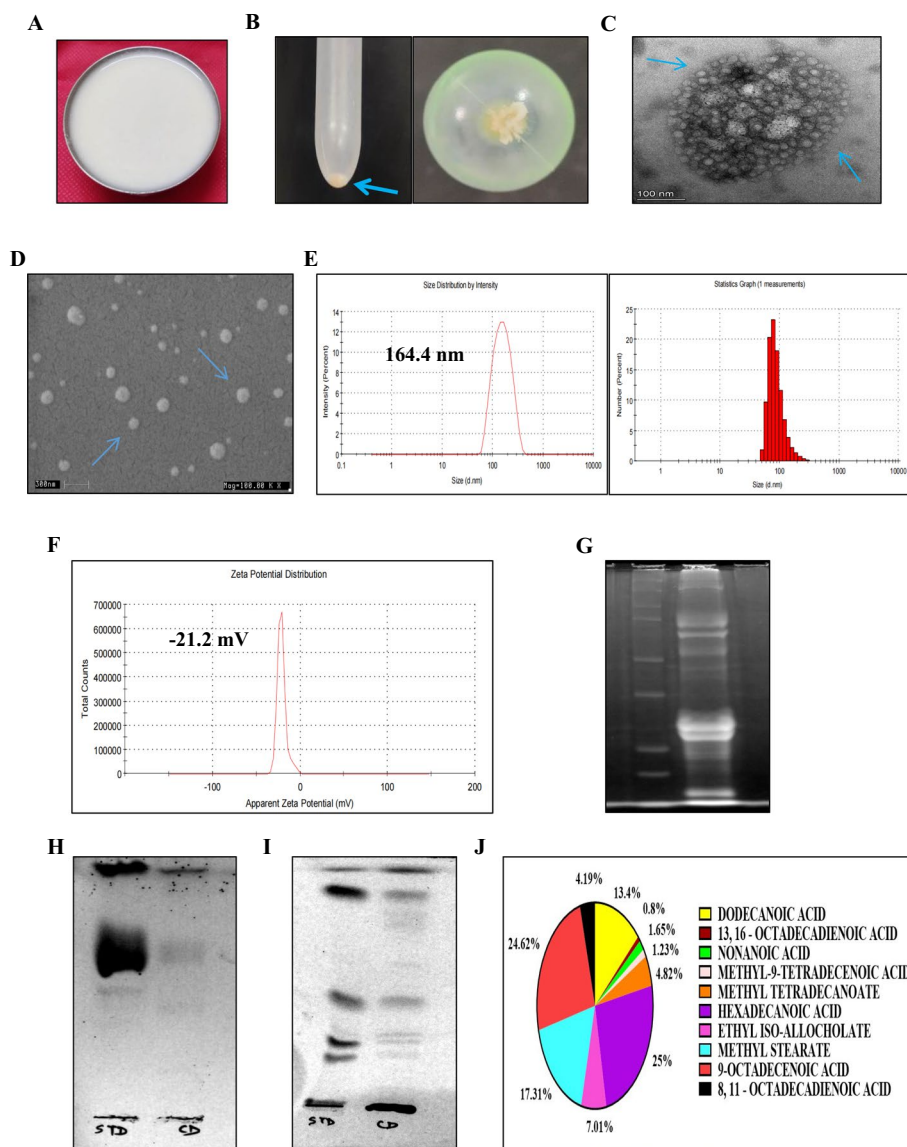


Fig. 1 **A** Curd prepared from cow milk. **B** Curd exosomes pellet. Characterisation of curd exosomes. **C** TEM image of curd exosomes. Scale bar: 100 nm. **D** SEM image of curd exosomes. Scale bar: 300 nm. **E** Zeta sizer measurements depict the size distribution in nm. **F** Zeta potential of curd exosomes by dynamic light scattering. **G** Exosomal protein content determination by SDS-PAGE. **H** The phospholipids band pattern was resolved on the TLC plate, showing faint bands. **I** Lipid determination in curd exosomes shows bands of neutral lipids on the TLC plate. **J** Quantitative analysis of major fatty acid content in curd exosomes by GC–MS, where each area in the pie chart shows the percentage relative intensity of fatty acid

curd exosomes by GC–MS and confirmed the presence of Hexadecanoic acid, Octadecenoic acid, Methyl stearate, Lauric acid, and Ethyl iso-allocholate at a significant level (Fig. 1J) (Additional file 1: Fig. S1).

These lipid markers were favourably reported in the research performed on the extracellular vesicles derived from human plasma (Liangsupree et al. 2022). Consequently, we figured that there could be a certain difference in characterisation values depending on the parental origin of exosomes.

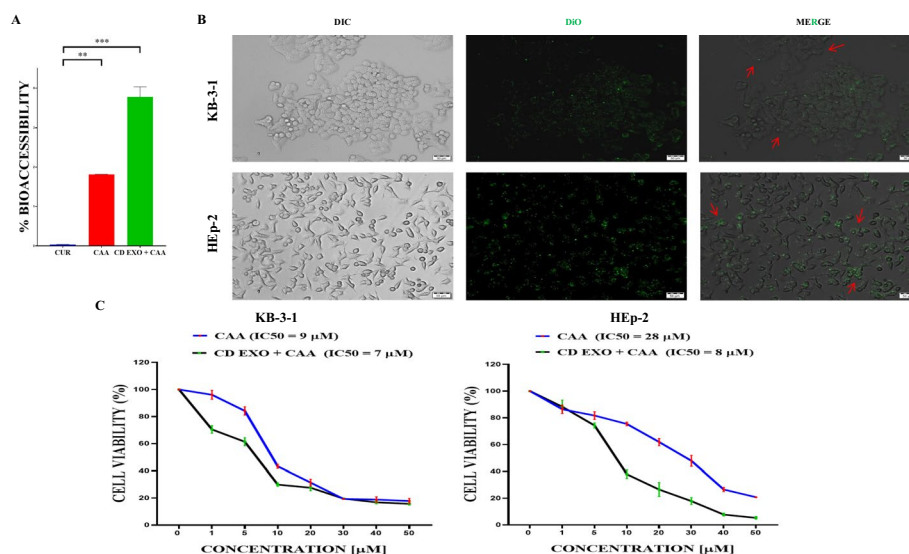


Fig. 2 **A** Comparative analysis of the bioaccessibility of curcumin, CAA, and CD EXO + CAA. The statistical analysis was carried out by a one-way ANOVA test with $n=3$. ($*P < 0.05$, $**P < 0.01$, $***P < 0.001$, $****P < 0.0001$). Bars indicate mean \pm SEM. **B** DiO-labelled exosomes interact with HNC cells. **C** The cell viability of KB-3-1 cells and HEp-2 cells treated with CAA and CD EXO + CAA was detected by MTT assay for 48 h. Graphs represent the mean \pm SEM for the cell viability experiment

Bioaccessibility of curcumin analogue alanine into curd exosomes

Bioaccessibility is the portion of food components absorbed by epithelial tissues after digestion that is usable by the cells and regulates their cellular processes. In the current study, the term was studied by utilising different digestive enzymes at different time intervals that mimic the conventional digestion processes in the body. Nevertheless, curcumin, found in nature, exhibits inferior bioaccessibility and lower solvability in aqueous medium and can be refined by certain transitions in their structure or by employing a delivery system (McClements and Xiao 2017). As part of this study, we performed a contrasting investigation of curcumin, CAA alone, and CAA loaded in curd exosomes evaluated by RP-HPLC. The HPLC chromatograms showed the presence of curcumin and CAA at a wavelength of 423 nm by the peak, with an identical retention time of 6 min. As shown in Fig. 2A, the result of HPLC indicated the revealed curcumin exhibited a minimum percentage bioaccessibility of 0.03435%, followed by CAA alone with 1.81458%, and CAA-loaded curd exosomes showed a higher value of 3.77664% with improved absorption. The nanoformulation secures CAA from any sort of degradation and facilitates easy delivery to the target site.

Targeting of curd exosomes into HNC cells

The analysis of an efficient targeting ability of curd exosomes in vitro on HNC cells. For that, KB-3-1 and HEp-2 cells were co-cultured with curd exosomes fluorescently labelled with DiO dye for 24 h of incubation. The co-cultured model was visualised by a fluorescent microscope, showing efficient interaction that helps in the convenient release of the drug along with its exosomal content into the target cells (Fig. 2B). Previous research reported that exosomes are used to convey their diverse components in

distinct tissues and cells and, therefore, serve as a messenger to carry out varied cellular processes in the body (Chen et al. 2021).

To validate the incorporation of CAA into curd exosomes by the sonication method, drug-loading capacity was estimated to be 3.992%, which depicts the quantity of CAA entered inside the exosomes by the total CAA taken for the incorporation, and entrapment efficiency was 11.975%. Former studies reported the drug incorporation into the nanovesicles by sonication method was suitable due to its efficient internalisation and the integrity of smaller nanovesicles remain intact (Colja et al. 2023).

Effect of curcumin analogue alanine on HNC cell proliferation

The inhibition of cell growth by CAA was determined in distinct quantities from 1 μM to 50 μM with a time interval of 24 and 48 h by MTT assay. The figure (Fig. 2C) depicts the growth inhibition curve for CAA alone and CAA-loaded exosomes, which were considered to be 9 μM and 7 μM , respectively, in KB-3-1 cells for 48 h. Similarly, the reduction in cell viability with CAA was found to be 28 μM , and CAA-loaded exosomes were 8 μM in HEp-2 cells for 48 h. The anti-proliferative effects increased by incorporating CAA into curd exosomes through better delivery to the tumour cells, thereby requiring a lesser concentration of the drug to inhibit 50% cell growth as compared with the free drug. Based on these observations, we selected these IC₅₀ values for further analysis. The MTT assay determines the healthy mitochondria that were affected by the drug, further reducing them to insoluble formazan (Ravi Shankara et al. 2016). CAA affects the mitochondria, inhibits the cell survival of tumour cells, and promotes apoptosis.

Deviation in FTIR spectrum of CAA in contrast with curcumin

FTIR exhibits the chemical properties of the compound by the presence of specific functional groups. Its peak intensity is related to the transmittance percentage corresponding to the functionality described in the sample for the wavenumber. FTIR spectra of curd exosomes differ from curcumin and its analogue at the 1067 cm^{-1} fingerprint area exhibiting asymmetrical stretching of aliphatic group vibrations. Moreover, there was a variation in the transmittance by the decrease in intensity at the range from 1039 to 1255 cm^{-1} fingerprint area indicating stretching of the carbonyl group, bending of alcohol vibrations, and C–N bonds in CAA and its nanoformulation in contrast with curcumin due to the conjugation of amino acid alanine. However, there were insignificant differences in the transmittance between CAA and its nano formulation since there were no changes in the chemical composition before and after loading in the curd exosomes. This finding indicated that transformation occurred at the synthesis level of the analogue from the conventional structure of curcumin (Fig. 3A). The former reports have mentioned the transformation in the configuration curcumin at the fingerprint area from 1000 to 1300 cm^{-1} (Vellampatti et al. 2018).

Influence of CAA on structural and nuclear change in HNC cells

To substantiate the impact of CAA on KB-3-1 and HEp-2 cells, the cells were treated for 48 h, and the morphology was examined using an inverted microscope. The untreated HNC cells multiply conventionally, forming colonies with epithelial morphology. On the other hand, the morphology was altered, with the majority of cells becoming round

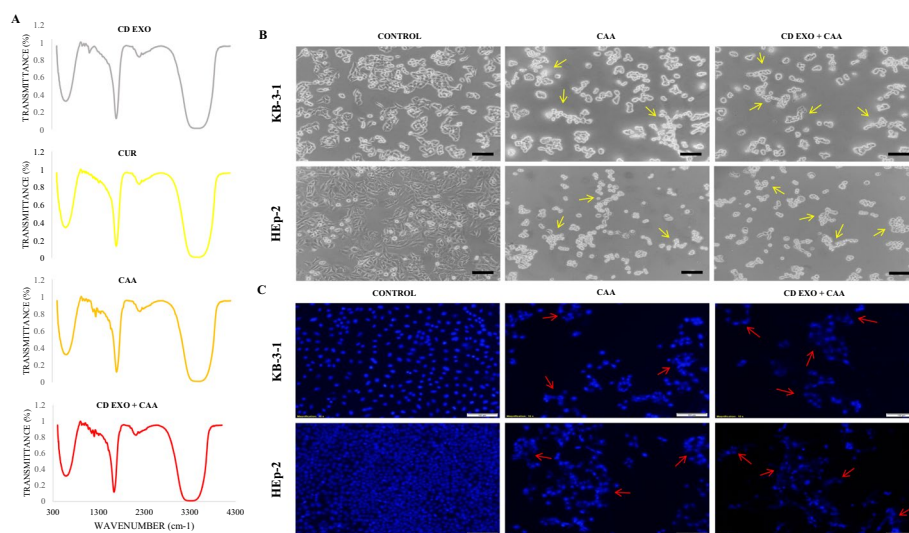


Fig. 3 **A** FTIR spectrum of CD EXO, CUR, CAA, and CD EXO + CAA in the transmission range from 400 to 4000 cm^{-1} . **B** The morphological changes were observed on KB-3-1 cells and HEP-2 cells treated with the IC50 concentrations of CAA and CD EXO + CAA for 48 h. Scale bar: 10X. **C** The nuclear fragmentation depicted by DAPI staining of KB-3-1 cells and HEP-2 cells after treatment with CAA and CD EXO + CAA. Scale bar: 10X

(Fig. 3B) and undergoing cytoplasmic blebbing in both treated groups. There were floating cells since the cells got detached, thereby losing their adherence ability. Therefore, we carefully observed significant differences in cell area among the control and treated groups; thus, CAA inhibits cell proliferation and causes cell death. Further experiments were performed to analyse nuclear morphology post-CAA treatment.

HNC cells were seeded on the plate, treated with CAA alone, and exosomes loaded CAA at their half-inhibitory concentrations for 48 h. DAPI staining is depicted in Fig. 3C. CAA causes nuclear condensation and cellular disintegration into apoptotic bodies. Therefore, the results of DAPI staining depicted disintegrated nuclei and a reduced cell population after the exposure of CAA to HNC cells.

CAA inhibits colony formation and encourages apoptosis in HNC cells

The influence of CAA on the vitality of cancer cells was investigated by a clonogenic assay. The result of the assay showed a significant decrease in the growth of cells that

(See figure on next page.)

Fig. 4 **A** CAA inhibits colony tumour cell colony formation in KB-3-1 and HEP-2 cells treated with the CAA and CD EXO + CAA, cultured, and colonies were counted. **B** Statistical analysis results of colony formation in KB-3-1 and HEP-2 cells. Bars indicate mean \pm SEM. **C** Western blot images of EphA2 and its associated molecules protein levels in KB-3-1 and HEP-2 cells target the EphA2 signalling mechanism. **D** Quantitative analysis of the protein expression of EphA2 *P*-value (0.0002 for KB-3-1 cells and 0.0012 for HEP-2 cells) and other molecules from normalised to β -actin with $n=3$. ($*P < 0.05$, $**P < 0.01$, $***P < 0.001$, $****P < 0.0001$). Bars indicate mean \pm SEM. **E** PCR results depicting relative mRNA expression of EphA2-related molecules on KB-3-1 cells and HEP-2 on agarose gel. **F** Quantitative analysis shows a significant change in mRNA expression of EphA2 *P*-value (0.0011 for KB-3-1 cells and 0.0002 for HEP-2 cells) and its related molecules on KB-3-1 cells and HEP-2 cells after treatment with CAA and CD EXO + CAA. A statistical study performed using multiple variance analysis (one-way ANOVA) with Tukey statistical analysis was done using a graph prism with $n=3$. ($*P < 0.05$, $**P < 0.01$, $***P < 0.001$, $****P < 0.0001$). Bars indicate mean \pm SEM

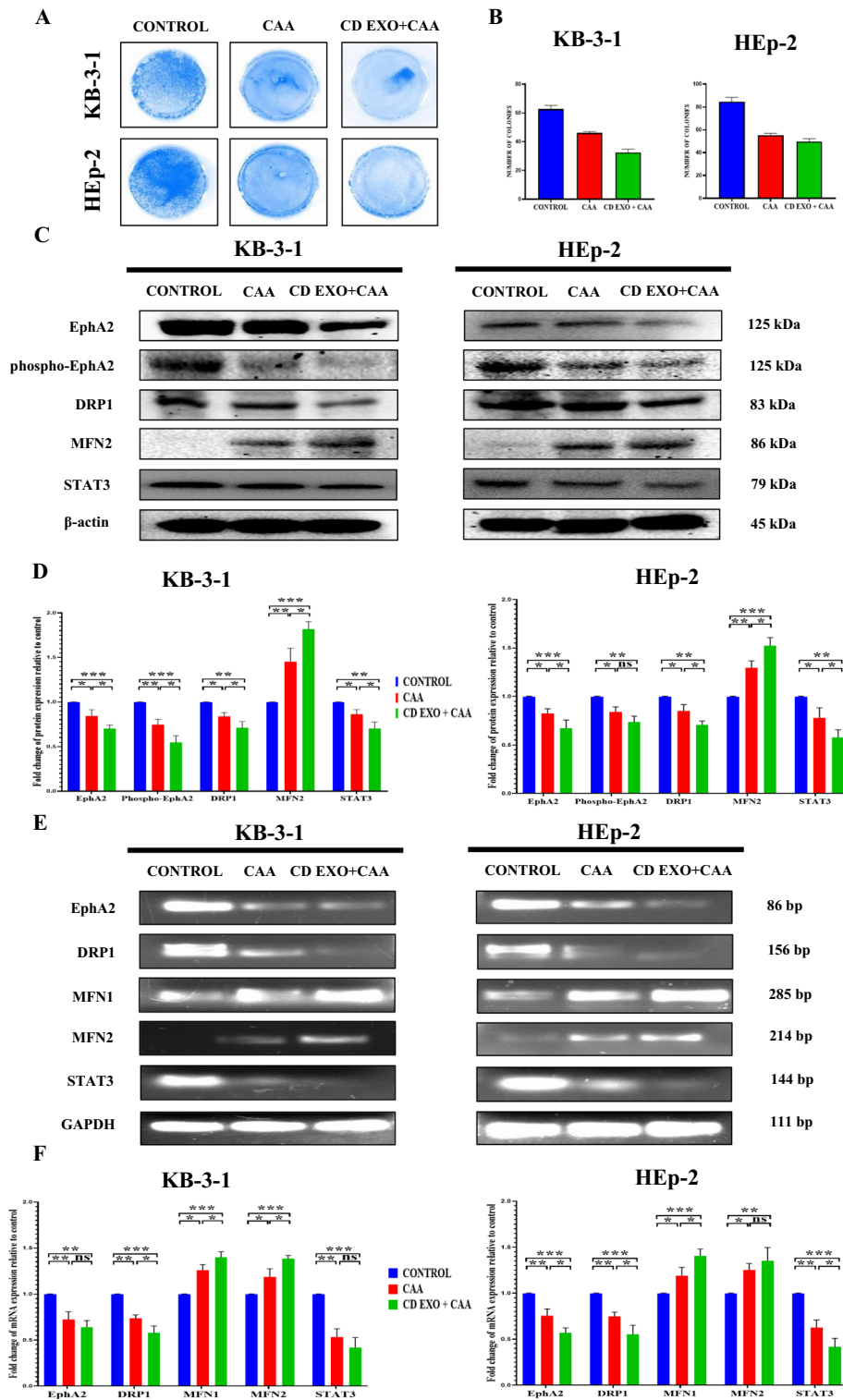


Fig. 4 (See legend on previous page.)

attenuated their colony-forming ability (Fig. 4A). Its effects showed poor growth status and cell division processes. Compared with the control group, the number of colonies was lower in both the treated groups of CAA alone and CAA loaded in exosomes.

The CAA alone treated showed 46 and 47 colonies, while the CAA loaded into curd exosomes treated showed 32 and 40 colonies for KB-3-1 and HEp-2 cells, respectively, after 48 h. In contrast, the untreated group depicted 63 and 58 colonies for KB-3-1 cells and HEp-2 cells, respectively, which are graphically represented in Fig. 4B. Accordingly, it became evident from the above results that the CAA-treated HNC cells displayed a reduction in tumour advancement.

To further investigate the functions of CAA on HNC cells, a dead-alive assay was performed. AO depicts live and dead cells; on the other hand, EtBr stained only apoptotic cells after entering the membrane. In our study, KB-3-1 cells and HEp-2 cells were seeded on the plates and treated with CAA alone or CAA loaded with curd exosomes. The treated cells undergoing apoptosis showed more red fluorescence in both groups, whereas the untreated group depicted green fluorescence, indicating healthy cells (Fig. 5A). The increased number of red fluorescence describes the apoptosis phenomenon since the treated cells lose their membrane integrity. Apoptosis allows an organised mechanism of cell death that engenders cell membrane contraction, leading to the loss of an intact framework, nuclear fragmentation, cytochrome C release from mitochondria, activation of caspases, and the formation of apoptotic bodies (Khader et al. 2020). Similarly, CAA significantly stimulates the apoptosis mechanism in HNC cells.

CAA targets the EphA2 signalling mechanism

EphA2 tyrosine kinase receptor had been known as epithelial cell kinase (Eck) and was related to diverse cytoplasmic as well as cell surface proteins (Lindberg and Hunter 1990). Its activation is commonly involved in nervous system development; however, it acts as a growth promoter by activating AKT and PKA, which favour lamellipodia expansion and are involved in the EMT mechanism and metastasis (Zhou and Sakurai 2017). In the present study, we measured the EphA2 level in HNC cells by western blotting. The result revealed that higher expression of EphA2 in untreated KB-3-1 cells and HEp-2 cells was reduced post-treatment with CAA after 48 h. Moreover, we observed a significant reduction of EphA2 in CAA loaded with curd exosomes with (95% of confidence interval = 0.2626–0.5099, adjusted P -value = 0.0002 for KB-3-1 cells and 95% of confidence interval = 0.1847–0.4685, adjusted P -value = 0.0010 for Hep-2 cells) as compared to the CAA alone (95% of confidence interval = 0.1366–0.3839, adjusted P -value = 0.0016 for KB-3-1 cells and 95% of confidence interval = 0.03064–0.3144, adjusted P -value = 0.0227 for Hep-2 cells). Likewise, the phosphorylated EphA2 level in cells treated with CAA (95% of confidence interval = 0.1153–0.3935, adjusted

(See figure on next page.)

Fig. 5 **A** CAA leads to apoptosis shown by the AO-EtBr assay using fluorescent microscopy merged images of KB-3-1 and HEp-2 cells after treatment with apoptosis-related CAA and CD EXO + CAA at their respective IC50 values. **B** Effect on apoptosis-related protein expression in KB-3-1 and HEp-2 cells treated with CAA and CD EXO + CAA for 48 h. β -Actin was used as a housekeeping molecule. **C** Graphical representation of relative protein expression of Caspase-7 and Bcl-xL with $n = 3$. (* $P < 0.05$, ** $P < 0.01$, *** $P < 0.001$). **D** Representative mRNA expression analysis in KB-3-1 and HEp-2 cells upon CAA and CD EXO + CAA was determined using PCR, where GAPDH was used as a housekeeping gene. **E** Statistical analysis showing mRNA expression of apoptosis-related molecules on KB-3-1 cells and HEp-2 cells after treatment with CAA and CD EXO + CAA. Statistical representation was done by one-way ANOVA with a Gaussian distribution by Tukey comparison test with $n = 3$. (* $P < 0.05$, ** $P < 0.01$, *** $P < 0.001$, **** $P < 0.0001$). Bars indicate mean \pm SEM

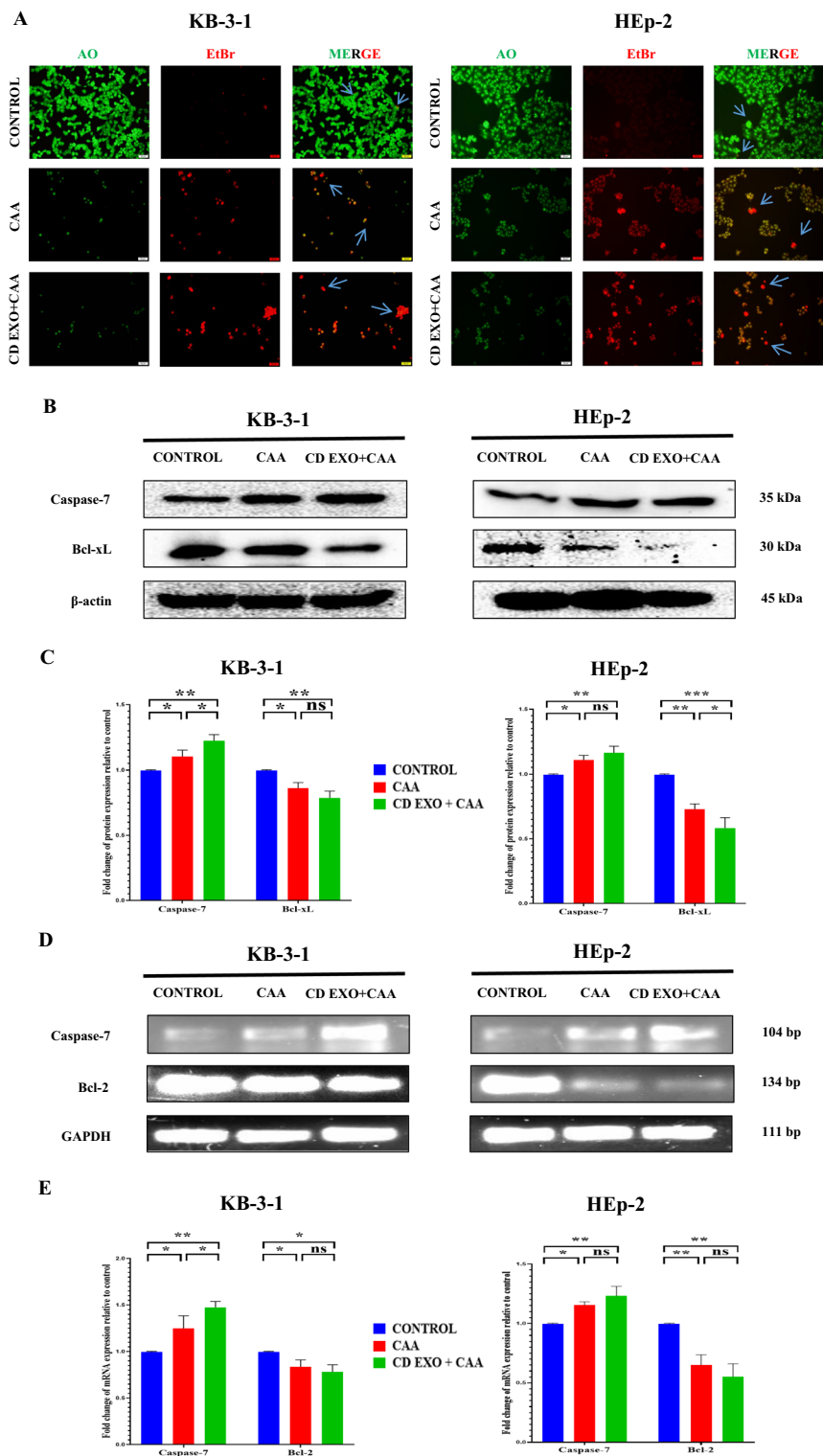


Fig. 5 (See legend on previous page.)

P -value=0.0033 for KB-3-1 cells and 95% of confidence interval=0.04143–0.2721, adjusted P -value=0.0139 for Hep-2 cells) and CAA loaded with curd exosomes (95% of confidence interval=0.3087–0.5869, adjusted P -value=0.0002 for KB-3-1 cells and

95% of confidence interval = 0.1469–0.3776, adjusted *P*-value = 0.0011 for Hep-2 cells) was declined. To evaluate whether CAA could regulate the mitochondrial dynamics mechanism, we analysed the expression of DRP1 involved in mitochondrial fission that got down-regulated by CAA; on the other hand, MFN2 mitochondrial fusion molecule expression got elevated (Fig. 4C, D). To understand the molecular mechanism that supports the CAA-dependent triggering of apoptosis and suppression of tumour augmentation in HNC cells, we examined the effect on STAT3 and cell death-related molecules. Interestingly, we observed a decrease in Bcl-xL expression but increased Caspase-7 in contrast with the control group, which revealed the inhibition of tumorigenesis and mediated apoptosis (Additional file 3: Table S1). Consequently, CAA promotes mitochondrial fusion, which further influences the apoptosis pathway (Fig. 5B, C) (Additional file 2: Fig. S2).

The investigation of EphA2 pathway by western blot was further confirmed by PCR. In the study, we found a clear decline in the mRNA expression of EphA2 in both treated groups compared with the control; the EphA2 level in cells treated with CAA (95% of confidence interval = 0.1130–0.4324, adjusted *P*-value = 0.0047 for KB-3-1 cells and 95% of confidence interval = 0.1095–0.3715, adjusted *P*-value = 0.0032 for Hep-2 cells) and CAA loaded with curd exosomes (95% of confidence interval = 0.1979–0.5173, adjusted *P*-value = 0.0011 for KB-3-1 cells and 95% of confidence interval = 0.2966–0.5586, adjusted *P*-value = 0.0001 for Hep-2 cells). Likewise, DRP1 and STAT3 levels were also lowered by the effects of the CAA-free drug and the exosome-loaded drug. Moreover, we noticed an up-regulation in the process of mitochondrial fusion molecules MFN1 and MFN2 (Fig. 4E, F), along with Caspase-7, in the treated groups (Fig. 5D, E) (Additional file 4: Table S2). The expression of Bcl-2 was also reduced in both treated groups. All these findings suggested that CAA could inhibit viability by targeting EphA2, followed by influencing transcription factor STAT3 and the mitochondrial dynamics process to induce apoptosis in KB-3-1 and Hep-2 cells.

Discussion

Head and neck squamous cell carcinomas are considered to be one of the most threatening diseases worldwide. In India, the male population has the highest incidence rate compared with females; it mainly arises due to processed meat, saturated fat, tobacco, and alcohol intake. HPV was reported as one of the causes of HNC and exhibits genetic modification in tumour suppressor p53, resulting in high chances of occurrence (Mishra 2009). Other factors, including Asbestos, the Epstein–Barr virus, Syphilis, and bad mouth cleaning habits, enhance the risk of HNC. Throat pain, swelling, tooth loss, and difficulty in food ingestion were the complications experienced by the patients. On this account, surgery, radiation, co-adjuvant therapy, and chemotherapy were performed based on the tumour site and stage, followed by the positioning of transgastric-jejunal (G–J) tubes into the mouth of the patient to provide dietary support for their survival (Hall and Koeller 1990). Field cancerization for HNC includes gene mutations resulting in the aggressive growth of cells that disperse from the oral mucosa to various organs. Therefore, the neoplastic cells lose their ability to regulate the cell cycle due to genomic variation; therefore, biomarker development appears necessary for the early detection of HNC among patients (Bansal et al. 2020). In general, HNC biology needs more

findings regarding cytosolic proteins driving mitochondrial mechanisms and metastasis processes for targeting tumorigenesis. The present study focussed on EphA2, a crucial tumour biomarker that is involved in the dual function of receptor and ligand-based cell signalling, its association with AKT/mTOR signalling on the one hand, and EGFR with Ephexin1 complex formation for tumour advancement on the other hand (Al-Jamaei et al. 2023). EPHA comprised nine members (EphA1–EphA8, EphA10) molecules involved in cellular communication by interacting with ligands outside the cells as well as intracellular proteins. The loss of heterozygosity is approximately 20%, along with higher expression in tumour tissues as compared with normal (Rivera et al. 2008). EphA2 was described as a biomarker of pancreatic cancer by interacting with MT1-MMP on the cell membrane, triggering MAPK signalling, and is found at a higher level in the sera of tumour patients (Koshikawa et al. 2017). The higher expression of EphA2 showed a lower 5-year survival rate of 29% and lymph node metastasis. The major localization found in the cell membrane and cytosol and activated by tyrosine phosphorylation, therefore, can be targeted for HNC (Miyazaki et al. 2003).

Exosomes are involved in intricate biological processes as a biomarker for cancer detection, as the nanocarriers for distinct molecules with the ability to induce an immune response. Recent research examined the function of exosomes as nanomedicine for the monkeypox virus by encapsulating the high-performance photothermal molecule (TPE-BT-DPTQ) in poly (lactic-co-glycolic acid) polymeric nanoparticles treated on macrophages. The biomimetic nanoparticles demonstrated anti-viral activity, and reduction of inflammation, ultimately promoting wound healing and preventing viral dissemination to other individuals (Li et al. 2024). Nanoscale covalent organic frameworks are regarded as beneficial for cancer therapeutic in the conveyance of drugs, such as curcumin, ibuprofen, captopril, and doxorubicin. Moreover, they exhibited advancement in gene therapy, chemodynamic therapy, and nanozyme-mediated tumour therapy (He et al. 2021). Human serum albumin-derived exosomes showed biocompatibility in the dried state and dissolved rapidly in the solvent for the treatment of different cancers. Albumin nanoparticles packed with cabazitaxel decreased the expression of TGF β , reduced tumour volume and acute toxicity in paclitaxel-resistant lung cancer (Tan et al. 2023). Moreover, the blood–brain barrier allows the selective transfer of ions and different molecules from the blood to the brain, therefore, is considered an important characteristic of the central nervous system. Exosomes have the potential to pass through the blood–brain barrier which could help in the observation of brain disorders, such as Alzheimer's, multiple sclerosis, and Parkinson's disease and further allow effective drug delivery to the endothelial cells and astrocytes (Salarpour et al. 2022).

Curd is comprised of high nutritional components, including vitamins, proteins, minerals, carbohydrates, fats, and metabolites. Moreover, they can be employed as a suitable probiotic for maintaining healthy gut microflora, countering peculiar allergies, and strengthening immunity (Sharma et al. 2017). The current investigation deals with nanovesicles isolated from curd taken as a medium for the transmission of a specific drug to the target cells to affect their conventional biological processes. Exosomes are considered a versatile class of extracellular vesicles that perform different functions based on their parental cell. Curd exosomes were isolated by the ultracentrifugation method and characterised using DLS for their average size (114.6 nm)

and zeta potential (-21.2 mV), followed by SDS-PAGE, which depicted a wide spectrum of exosomal proteins. TEM and SEM depicted the spherical morphology of curd exosomes. Its lipid content, determined by TLC and GC-MS, depicted phospholipids, neutral lipids, and fatty acids, which include dodecanoic acid, hexadecanoic acid, methyl stearate, and ethyl iso-allocholate. These results confirmed the exosomes isolated from curd by an appropriate procedure with promising representation in the similar manner mentioned in previous reports (Fakhredini et al. 2022; Skotland et al. 2019; Liangsupree et al. 2022). It is essential to identify the different lipids present in exosomes to understand their role in cell metabolism and various biological processes.

Curcumin has become a highlighted topic of research in the field of remedial medicine and the overall well-being of the population. Curcumin can be explained as a polyphenolic compound first isolated in 1815 and its structure deduced in 1910; though, its description and application were mentioned in Ayurveda around 5000 years ago (Sharifi-Rad et al. 2020). Curcumin is lipophilic and stable in its solid state, with a molecular weight of 368.39 g/mol; however, its attachment of amino acids results in a slight difference in its weight of 510.20 g/mol. Its structural transformation brings out a difference in its assorted capabilities due to its blocking of the hydrogen atom transfer mechanism by amino acid alanine, which affects ROS scavenging activity at 0.055 μ M for alanine and the anti-oxidant activity of the analogue by 57% less than curcumin (Parvathy et al. 2010). The curcumin analogue Alanine was loaded into exosomes using the sonication method. On this account, the identification of CAA inside curd exosomes was determined with an efficient drug-loading capacity of 3.992% and an entrapment efficiency of 11.975%. Furthermore, the potent drug delivery into the target cells was studied with Exo-DiO fluorescent dye incubation. The uptake of exosomes was observed, depicting the adherence of exosomes to the surface of tumour cells that allows the merging of the membranes, followed by the release of exosomal content into the cytosol. The exosomes were identified as interacting with the recipient cells by the endocytosis mechanism, which allows clathrin and caveolin molecules to facilitate subsequent internalisation with Rab, RhoA, and dynamin proteins (Joshi et al. 2020; McKelvey et al. 2015).

Curcumin is a powerful antidote that prevents numerous ailments in the entire body when consumed orally or applied directly to the skin. Despite that, curcumin is still anticipated for FDA approval when it comes to the prevention of various cancers (PDQ Cancer Information 2023). In the present study, we discussed curcumin, a bioactive ingredient present in turmeric, and its analogue Alanine, which was synthesised by the conjugation of the amino acid Alanine with the basic structure of curcumin. Its chemical bonds modified at the fingerprint region in the range from 1039 to 1255 cm^{-1} by attaching alanine amino acid revealed in FTIR spectrum analysis. Curcumin still faced shortcomings of low aqueous solubility and absorption capacity; therefore, in this study, we compared its intake strength after consequent treatment of digestive enzymes from the analogue CAA along with its exosome-loaded composition. Therefore, we analysed the bioaccessibility of CAA and its exosomes formulation, which was compared with curcumin, which was higher in CAA (1.814585545%), which got further enhanced in curd exosomes loaded CAA (3.776649802%). Curd

exosomes indicate an improved absorption process and allow higher release of CAA from the matrix and solubilization. The result suggested that CAA exhibits better assimilation potential, and the strategy to incorporate the analogue in exosomes proved to enhance curcumin potency.

Moving forward towards the influence of CAA on HNC cells, the cytotoxicity assay showed a reduction in growth depending on the concentration. Among the HNC cell lines KB-3-1 and HEp-2 treated for 48 h, we observed a better impact of CAA when delivered via curd exosomes because of its reduced IC₅₀ value evaluated against CAA alone. This indicated that CAA encapsulated in exosomes has conveniently entered the target cells and can influence their metabolism at a lesser concentration. Thereby exhibiting a similar effect of half-growth inhibition in comparison with a higher concentration of the CAA-free drug. Curcumin is a hydrophobic compound; however, the combination with amino acids in the form of analogue has improved its solubility and easy access into the HNC cells. Increase in DNA fragmentation in CAA-treated HNC cells and inhibit cell proliferation, resulting in a lesser number of colonies. The results of the AO-EtBr assay also indicated regulated cell death by the treatment with CAA, which was more prominent in the exosomes loaded CAA group. In this context, we analysed whether the expression of EphA2 and STAT3 was significantly decreased after the treatment of CAA and its nano formulation for 48 h in HNC cells. EphA2 influences the expression of STAT3 since its knockdown down-regulates STAT3 levels in hepatocellular carcinoma. It inhibits the phosphorylation of STAT3 at the tyrosine 705 residue and prevents tumour growth (Wang et al. 2021a, 2021b). In particular, we further examined the salient markers of mitochondrial dynamics, it seemed CAA promoted the fusion mechanism by strengthening MFN1 and MFN2 molecules; on the other hand, there was a reduction in DRP1 expression inhibiting mitochondrial fission. Moreover, there was a significant difference in the expression level affected by the targeted delivery of CAA through curd exosomes, which increased its concentration inside the tumour cells and consequently advanced the curative effect. Inhibition of STAT3 leads to a decrease in DRP1 transcription, resulting in apoptosis of tumour cells (Guo et al. 2024). The optimistic result of increasing trends in the expression of Caspase-7, along with suppression of Bcl-2 and Bcl-xL was observed by the treatment of CAA, and its nanoformulation tends to accelerate the apoptosis mechanism. Former reports depicted curcumin emerging as an anti-cancer drug targeting various malignancies (Xi et al. 2015); similarly, we found CAA triggers the cell death pathway and allows enhanced accessibility with a better effect on tumour cells.

Impressively, our comprehensive results showed that CAA could prevent cell viability and promote apoptosis in KB-3-1 and HEp-2 HNC cells. Furthermore, curd exosomes that allowed targeted conveyance of CAA proved to be a favourable carrier platform against cancer advancement.

Conclusion

There were numerous research articles related to the anti-tumour activity of curcumin in the majority of types of cancer, but this was the primary study to analyse the effect of curcumin analogue Alanine on HNC cells. Our investigation showed that CAA has better bioaccessibility than curcumin, and in addition, its ability gets enhanced when served

through curd exosomes. CAA induced an anti-tumour impression in KB-3-1 and HEp-2 cells by impeding EphA2 signalling through the STAT3-DRP1-MFN1/2 pathway and enhancing the expression of caspases supporting apoptosis. Nonetheless, there is a limitation in the current analysis that in vivo experiments are required. Henceforth, future research is essential for constructing anti-cancer drug formulations against metastasis.

Abbreviations

HNC	Head and neck cancer
CUR	Curcumin
CAA	Curcumin analogue alanine
CD EXO	Curd exosomes
EphA2	Erythropoietin-producing hepatocellular receptor 2 or Ephrin type-A receptor 2
PBS	Phosphate buffer saline

Supplementary Information

The online version contains supplementary material available at <https://doi.org/10.1186/s12645-024-00286-y>.

Additional file 1.

Additional file 2.

Additional file 3.

Additional file 4.

Acknowledgements

The authors acknowledge the support of the Director, CSIR-Central Food Technological Research Institute, Mysore, India.

Author contributions

KP and AK designed the research work. KP carried out the experiments, analysis, and manuscript writing. BBK provided technical expertise, review and resources. AK acquired funding, investigation, provided the resources, validated the results and revised the manuscript. All authors read and approved the final manuscript.

Funding

This study was financially supported by the DST-SERB (ECR/2018/000894) and CSIR-CFTRI, India.

Availability of data and materials

No datasets were generated or analysed during the current study.

Declarations

Ethics approval and consent to participate

Not applicable.

Consent for publication

All the authors agree to the publication of this manuscript.

Competing interests

The authors declare no competing interests.

Received: 21 February 2024 Accepted: 14 August 2024

Published online: 18 September 2024

References

- Aggarwal BB, Sundaram C, Malani N et al (2007) Curcumin: the Indian solid gold. *Adv Exp Med Biol* 595:1–75
- Al-Jamaei AAH, Subramanyam RV, Helder MN et al (2023) A narrative review of the role of Eph receptors in head and neck squamous cell carcinoma. *Oral Dis*. <https://doi.org/10.1111/odi.14625>
- Ansari FJ, Tafti HA, Amanzadeh A (2024) Comparison of the efficiency of ultrafiltration, precipitation, and ultracentrifugation methods for exosome isolation. *Biochem Biophys Rep* 38:101668
- Anubala S, Sekar R, Nagaiah K (2014) Development and validation of an analytical method for the separation and determination of major bioactive curcuminoids in *Curcuma longa* rhizomes and herbal products using non-aqueous capillary electrophoresis. *Talanta* 123:10–17
- Ashrafizadeh M, Kumar AP, Aref AR et al (2022) Exosomes as promising nanostructures in diabetes mellitus: from insulin sensitivity to ameliorating diabetic complications. *Int J Nanomed* 17:1229–1253

- Bagal S, Budukh A, Singh TJ et al (2023) Head and neck cancer burden in India: an analysis from published data of 37 population-based cancer registries. *Ecancer*. 17:1603
- Bajaj KK, Chavhan V, Raut NA et al (2022) Panchgavya: A precious gift to humankind. *J Ayurveda Integr Med* 13(2):100525
- Balaganesh S, Kumar P, Girija ASS et al (2022) Probiotic curd as antibacterial agent against pathogens causing oral deformities—in vitro microbiological study. *J Adv Pharm Technol Res* 13(Suppl 2):S510–S513
- Bansal R, Nayak BB, Bhardwaj S et al (2020) Cancer stem cells and field cancerization of head and neck cancer—an update. *J Family Med Prim Care* 9(7):3178–3182
- Barchitta M, Maugeri A, Favara G et al (2019) Nutrition and wound healing: an overview focusing on the beneficial effects of Curcumin. *Int J Mol Sci* 20(5):1119
- Caron C, Bertolin G (2024) Cristae shaping and dynamics in mitochondrial function. *J Cell Sci* 137(1):260986
- Chen H, Wang L, Zeng X et al (2021) Exosomes, a new star for targeted delivery. *Front Cell Dev Biol* 9:751079
- Cohen N, Fedewa S, Chen AY (2018) Epidemiology and demographics of the head and neck cancer population. *Oral Maxillofac Surg Clin North Am* 30(4):381–395
- Colja S, Jovčevska I, Šamec N et al (2023) Sonication is a suitable method for loading nanobody into glioblastoma small extracellular vesicles. *Heliyon* 9(5):e15674
- Counihan J, Fried B, Sherma J (2010) Effects of *Echinostoma caproni* infection on the neutral and polar lipids of intestinal and non-intestinal organs in the BALB/c mouse as determined by high-performance thin-layer chromatography. *Parasitol Res* 107(4):947–953
- Curcumin market size and share analysis - growth trends & forecasts (2023–2028)
- Dundar AN, Uzuner K, Parlak ME et al (2022) Enhanced functionality and bio-accessibility of composite pomegranate peel extract-Enriched "Boba Balls." *Foods* 11(23):3785
- Fakhredini F, Mansouri E, Mard SA et al (2022) Effects of exosomes derived from kidney tubular cells on diabetic nephropathy in rats. *Cell J* 24(1):28–35
- Fang KP, Zhang JL, Ren YH et al (2014) Talin-1 correlates with reduced invasion and migration in human hepatocellular carcinoma cells. *Asian Pac J Cancer Prev* 15(6):2655–2661
- Feng X, Chen X, Zheng X et al (2021) Latest trend of milk derived exosomes: cargos, functions, and applications. *Front Nutr* 8:747294
- Finney AC, Scott ML, Reeves KA et al (2021) EphA2 signaling within integrin adhesions regulates fibrillar adhesion elongation and fibronectin deposition. *Matrix Biol* 103–104:1–21
- Folch J, Lees M, Sloane Stanley GH (1957) A simple method for the isolation and purification of total lipids from animal tissues. *J Biol Chem* 226(1):497–509
- Folz BJ, Silver CE, Rinaldo A et al (2008) An outline of the history of head and neck oncology. *Oral Oncol* 44(1):2–9
- Frederik WM, Broekhoven S (1978) Separation and determination of lipids by one-dimensional micro-thin-layer chromatography followed by densitometry. *J Chromatogr A* 150(1):171–177
- Guo YW, Zhu L, Duan YT et al (2024) Ruxolitinib induces apoptosis and pyroptosis of anaplastic thyroid cancer via the transcriptional inhibition of DRP1-mediated mitochondrial fission. *Cell Death Dis* 15(2):125
- Gurung S, Perocheau D, Touramanidou L et al (2021) The exosome journey: from biogenesis to uptake and intracellular signalling. *Cell Commun Signal* 19(1):47
- Haji Mazdarani M, Jafarikia M, Nemati F (2019) Investigation of indolamine 2, 3 dioxygenase (IDO-1) gene expression by real-time PCR among patients with lung cancer. *J Cell Physiol* 234(8):13781–13787
- Hall P, Koeller J (1990) Head and neck cancer: detection and therapeutics. *Am Pharm NS* 30(4):28–32
- He X, Jiang Z, Akakuru OU et al (2021) Nanoscale covalent organic frameworks: from controlled synthesis to cancer therapy. *Chem Commun (Camb)* 57(93):12417–12435
- Irie N, Takada Y, Watanabe Y et al (2009) Bidirectional signaling through ephrinA2-EphA2 enhances osteoclastogenesis and suppresses osteoblastogenesis. *J Biol Chem* 284(21):14637–14644
- Joshi BS, de Beer MA, Giepmans BNG et al (2020) Endocytosis of extracellular vesicles and release of their cargo from endosomes. *ACS Nano* 14(4):4444–4455
- Kaidar-Person O, Gil Z, Billan S (2018) Precision medicine in head and neck cancer. *Drug Resist Updat* 40:13–16
- Keelery S (2023) Estimated production volume of turmeric in India FY 2023 by state. *Statistica India*
- Khader SZA, Syed Zameer Ahmed S, Ganesan GM et al (2020) Rhynchosia rufescens AgNPs enhance cytotoxicity by ROS-mediated apoptosis in MCF-7 cell lines. *Environ Sci Pollut Res Int* 27(2):2155–2164
- Khushboo KA, Malik T (2023) Characterization and selection of probiotic lactic acid bacteria from different dietary sources for development of functional foods. *Front Microbiol* 14:1170725
- Koshikawa N, Minegishi T, Kiyokawa H et al (2017) Specific detection of soluble EphA2 fragments in blood as a new biomarker for pancreatic cancer. *Cell Death Dis* 8(10):e3134
- Kubatka P, Koklesova L, Mazurakova A et al (2024) Cell plasticity modulation by flavonoids in resistant breast carcinoma targeting the nuclear factor kappa B signaling. *Cancer Metastasis Rev* 43(1):87–113
- Li B, Wang W, Zhao L et al (2024) Aggregation-induced emission-based macrophage-like nanoparticles for targeted photothermal therapy and virus transmission blockage in Monkeypox. *Adv Mater (deerfield Beach, Fla.)* 36(9):e2305378
- Liangsupree T, Multia E, Saarinen J et al (2022) Raman spectroscopy combined with comprehensive gas chromatography for label-free characterization of plasma-derived extracellular vesicle subpopulations. *Anal Biochem* 647:114672
- Lindberg RA, Hunter T (1990) cDNA cloning and characterization of eck, an epithelial cell receptor protein-tyrosine kinase in the eph/elk family of protein kinases. *Mol Cell Biol* 10(12):6316–6324
- Liu W, Zhai Y, Heng X et al (2016) Oral bioavailability of curcumin: problems and advancements. *J Drug Target* 24(8):694–702
- McClements DJ, Xiao H (2017) Designing food structure and composition to enhance nutraceutical bioactivity to support cancer inhibition. *Semin Cancer Biol* 46:215–226
- McKelvey KJ, Powell KL, Ashton AW et al (2015) Exosomes: mechanisms of uptake. *J Circ Biomark* 4:7
- Midekessa G, Godakumara K, Ord J et al (2020) Zeta potential of extracellular vesicles: toward understanding the attributes that determine colloidal stability. *ACS Omega* 5(27):16701–16710
- Miranda-Galvis M, Loveless R, Kowalski LP et al (2021) Impacts of environmental factors on head and neck cancer pathogenesis and progression. *Cells* 10(2):389

- Mirzaei S, Gholami MH, Aghdaei HA et al (2023) Exosome-mediated miR-200a delivery into TGF- β -treated AGS cells abolished epithelial–mesenchymal transition with normalization of ZEB1, vimentin and Snail1 expression. *Environ Res* 231(1):116115
- Mishra A (2009) Head and neck cancer in India–review of practices for prevention policy. *Oral Dis* 15(7):454–465
- Miyazaki T, Kato H, Fukuchi M et al (2003) EphA2 overexpression correlates with poor prognosis in esophageal squamous cell carcinoma. *Int J Cancer* 103(5):657–663
- Nguyen T, Aparicio M, Saleh MA (2015) Accurate mass GC/LC–quadrupole time of flight mass spectrometry analysis of fatty acids and triacylglycerols of spicy fruits from the apiaceae family. *Molecules* 20(12):21421–21432
- Okada K, Kato J, Miyazaki T et al (2009) The evaluation of the curd forming ability of milk replacers. *Anim Sci J* 80(1):12–18
- PDQ integrative, alternative, and complementary therapies editorial board (2023) Curcumin (Curcuma, turmeric) and cancer (PDQ[®]): patient version. In: PDQ Cancer Information Summaries National Cancer Institute (US)
- Parvathy KS, Negi PS, Srinivas P (2010) Curcumin–amino acid conjugates: synthesis, antioxidant and antimutagenic attributes. *Food Chem* 120(2):523–530
- Paskeh MDA, Entezari M, Mirzaei S et al (2022) Emerging role of exosomes in cancer progression and tumor microenvironment remodeling. *J Hematol Oncol* 15(1):83
- Patterson RH, Fischman VG, Wasserman I et al (2020) Global burden of head and neck cancer: economic consequences, health, and the role of surgery. *Otolaryngol Head Neck Surg* 162(3):296–303
- Porro C, Panaro MA (2023) Recent progress in understanding the health benefits of Curcumin. *Molecules* 28(5):2418
- Ravi Shankara BE, Ramachandra YL, Rajan SS et al (2016) Evaluating the Anticancer Potential of Ethanolic Gall Extract of *Terminalia chebula* (Gaertn.) Retz (Combretaceae). *Pharmacogn Res*. 8(3):209–212
- Rivera RS, Gunduz M, Nagatsuka H et al (2008) Involvement of EphA2 in head and neck squamous cell carcinoma: mRNA expression, loss of heterozygosity and immunohistochemical studies. *Oncol Rep* 19(5):1079–1084
- Salarpour S, Barani M, Pardakhty A et al (2022) The application of exosomes and exosome-nanoparticle in treating brain disorders. *J Mol Liq* 350:118549
- Sedykh SE, Purvinish LV, Monogarov AS et al (2017) Purified horse milk exosomes contain an unpredictable small number of major proteins. *Biochim Open* 4:61–72
- Shariati Najafabadi S, Amirpour N, Amini S et al (2021) Human adipose derived stem cell exosomes enhance the neural differentiation of PC12 cells. *Mol Biol Rep* 48(6):5033–5043
- Sharifi-Rad J, Rayess YE, Rizk AA et al (2020) Turmeric and its major compound curcumin on health: bioactive effects and safety profiles for food, pharmaceutical, biotechnological and medicinal applications. *Front Pharmacol* 11:01021
- Sharma C, Singh BP, Thakur N et al (2017) Antibacterial effects of Lactobacillus isolates of curd and human milk origin against food-borne and human pathogens. *3 Biotech* 7(1):31
- Skotland T, Hessvik NP, Sandvig K et al (2019) Exosomal lipid composition and the role of ether lipids and phosphoinositides in exosome biology. *J Lipid Res* 60(1):9–18
- Sun J, Zhang C, Bao YL et al (2014) Parthenolide-induced apoptosis, autophagy and suppression of proliferation in HepG2 cells. *Asian Pac J Cancer Prev* 15(12):4897–4902
- Sun L, Cao J, Chen K et al (2019) Betulinic acid inhibits stemness and EMT of pancreatic cancer cells via activation of AMPK signaling. *Int J Oncol* 54(1):98–110
- Tan T, Feng Y, Wang W et al (2023) Cabazitaxel-loaded human serum albumin nanoparticles combined with TGF β -1 siRNA lipid nanoparticles for the treatment of paclitaxel-resistant non-small cell lung cancer. *Cancer Nano* 14:70
- Teekaraman D, Elayapillai SP, Viswanathan MP et al (2019) Quercetin inhibits human metastatic ovarian cancer cell growth and modulates components of the intrinsic apoptotic pathway in PA-1 cell line. *Chem Biol Interact* 300:91–100
- Thiagarajan R, Manikandan R (2013) Antioxidants and cataract. *Free Radic Res* 47(5):337–345
- Vellampatti S, Chandrasekaran G, Mitta SB et al (2018) Metallo-curcumin-conjugated DNA complexes induces preferential prostate cancer cells cytotoxicity and pause growth of bacterial cells. *Sci Rep* 8(1):14929
- Wang H, Hou W, Perera A et al (2021a) Targeting EphA2 suppresses hepatocellular carcinoma initiation and progression by dual inhibition of JAK1/STAT3 and AKT signaling. *Cell Rep* 34(8):108765
- Wang J, Tang W, Yang M et al (2021b) Inflammatory tumor microenvironment responsive neutrophil exosomes-based drug delivery system for targeted glioma therapy. *Biomaterials* 273:120784
- Wu N, Li J, Luo H et al (2021) Hydroxysafflor yellow A promotes apoptosis via blocking autophagic flux in liver cancer. *Biomed Pharmacother* 136:111227
- Xi Y, Gao H, Callaghan MU et al (2015) Induction of BCL2-interacting killer, BIK, is mediated for anti-cancer activity of curcumin in human head and neck squamous cell carcinoma cells. *J Cancer* 6(4):327–332
- Xiao T, Xiao Y, Wang W et al (2020) Targeting EphA2 in cancer. *J Hematol Oncol* 13(1):114
- Yang Y, Shen G, Wang H et al (2018) Interferometric plasmonic imaging and detection of single exosomes. *Proc Natl Acad Sci USA* 115(41):10275–10280
- Yang ZJ, Zhang LL, Bi QC et al (2021) Exosomal connexin 43 regulates the resistance of glioma cells to temozolomide. *Oncol Rep* 45(4):44
- Yuan Y, Zhang S, Ma M et al (2022) Delivery of curcumin by shellac encapsulation: Stability, bioaccessibility, freeze-dried redispersibility, and solubilization. *Food Chem X* 15:100431
- Zhang YM, Liu YQ, Liu D et al (2019) The effects of astragalus polysaccharide on bone marrow-derived mesenchymal stem cell proliferation and morphology induced by A549 lung cancer cells. *Med Sci Monit* 25:4110–4121
- Zhao Z, Xie M, Li Y et al (2015) Formation of curcumin nanoparticles via solution-enhanced dispersion by supercritical CO₂. *Int J Nanomedicine* 10:3171–3181
- Zhou Y, Sakurai H (2017) Emerging and diverse functions of the EphA2 noncanonical pathway in cancer progression. *Biol Pharm Bull* 40(10):1616–1624

Publisher's Note

Springer Nature remains neutral with regard to jurisdictional claims in published maps and institutional affiliations.